JOURNAL OF THERMOPHYSICS AND HEAT TRANSFER
Vol. 13, No. 1, January–March 1999

Transient Heat Transfer in a Scattering–Radiating–Conducting Layer

Chengcai Yao* and B. T. F. Chung†
University of Akron, Akron, Ohio 44325-3903

Transient temperature distribution across a cooling semitransparent layer is obtained by using a direct numerical technique. The layer is emitting, absorbing, isotropically scattering, and heat conducting with a refractive index greater than or equal to one. The layer is cooled by radiation to a much colder environment. The solution involves simultaneously solving the transient energy equation using an implicit finite volume scheme and solving the integral equation for the radiative heat flux using the singularity subtraction technique and Gaussian numerical quadrature. Scattering is found to have a significant effect on the transient temperature distribution and the transient mean temperature of the layer.

Nomenclature

D = thickness of the medium, m
E_1, E_2, E_3 = the exponential integral functions, $E_n(x) = \int_0^1 \mu^{n-2} \exp(-x/\mu)\, d\mu$
G = incidence radiation, W/m^2
J_1, J_2 = radiosity from the interior of the two boundaries, W/m^2
$\bar{J}_1, \bar{J}_2$ = dimensionless radiocities, $J_1/\sigma T_0^4$, $J_2/\sigma T_0^4$
k = thermal conductivity of the medium, W/m-K
N = conduction–radiation parameter, $k/4\sigma T_0^3 D$
n = refractive index of the medium
T = absolute temperature, K
t = time, s
T_e = temperature of the surroundings, K
T_m = mean temperature, K
T_0 = initial temperature, K
X = dimensionless coordinate, x/D
x = coordinate in direction across the layer, m
α = absorption coefficient of the layer, m^{-1}
β = extinction coefficient of the layer, m^{-1}
θ = dimensionless temperature, T/T_0
θ_m = dimensionless mean temperature, T_m/T_0
κ_D = optical thickness of the layer, βD
ρ = interface reflectivity
ρc_p = product of density and specific heat of the layer, J/m^3-K
σ = Stefan–Boltzmann constant
τ = dimensionless time, $(4\sigma T_0^3/\rho c_p D)t$
ϕ = dimensionless incidence radiation, $G/\sigma T_0^4$
ω = scattering albedo

Introduction

THE transient thermal behavior of a single and multiple layer of semitransparent materials has been studied for a variety of cases, as reviewed recently by Siegel.[1] Many studies in the existing literature, however, are attributed to a medium of refractive index equal to one and with the medium bounded by walls with specified temperatures. In many applications involving ceramic components and coatings, crystal growth, laser processing of semiconductors, high-temperature solar energy applications, etc., the semitransparent materials are subjected directly to radiative and convective cooling or heating. When the refractive index is greater than one, the internal reflection from the interfaces must be taken into account. Some of the recent studies on transient thermal process in a semitransparent medium with radiative or convective boundary conditions are briefed in the following. Only a limited number of studies have considered the effect of refractive indices.

Tan and Lallemand[2] and Tan et al.[3] examined the transient temperature distribution in a glass plate subjected to various boundary conditions. A zone type of method was used to evaluate the radiative heat flux. Some comments on the effects of the refractive index were made, but scattering was not considered. A cylinder geometry suddenly exposed to a cold rarefied environment was analyzed by Baek et al.[4] A finite difference method and a discrete ordinate method were used to solve the energy equation and the radiative transfer equation, respectively. The effect of isotropic scattering was included. A multilayered geometry was considered by Tsai and Nixon,[5] and scattering was not included in their study. Hahn et al.[6] examined the transient heat transfer in a layer of ceramic powder during laser-flash measurements of thermal diffusivity. A three-flux method was used to solve the equation of radiative transfer. However, no results were presented on the effects of scattering and refractive indices.

Diaz and Viskanta[7] studied the melting of a semitransparent slab caused by an external radiation source. Highly peaked forward scattering was assumed for the radiation problem, and the radiation from the medium was neglected. The similar problems were also investigated by Seki et al.[8] and Nishimura et al.[9] Transient and steady combined conduction and radiation heat transfer in porous materials heated by highly concentrated solar radiation was examined by Matthews et al.[10]; a two-flux method was used to solve the radiative part of the problem. The transient heating of an absorbing–emitting–scattering material under direct radiation with different backplate boundary conditions was studied by Yuen and Khatami[11]; a semi-explicit finite difference technique was used to generate the numerical solutions.

The transient cooling of a layer of liquid drops was examined by Siegel[12] relative to the design of a radiator to dissipate heat in the outer space. A finite difference procedure was developed to obtain a highly accurate temperature distribution across the layer. The method was later extended to include the effect of large refractive indices,[13] and with more general boundary conditions.[14] However, the effect of scattering was not considered in these studies. Transient spectral radiation in a two-layer semitransparent composite was examined by Siegel[15] using the two-flux method to solve the radiative transfer

Received March 23, 1998; revision received June 29, 1998; accepted for publication June 29, 1998.

*Graduate Assistant, Department of Mechanical Engineering.
†F. Theodore Harrington Professor, Department of Mechanical Engineering.

equation. Isotropic scattering and effect of refractive indices were taken into account in this study.

The solution of the exact radiative transfer equation is rather complicated, particularly when the scattering is present; hence, a common approach is to use approximate methods such as the two-flux method and diffusion and differential approximations. Unfortunately, approximate methods are usually subject to certain constraints. For certain conditions, the methods may not be valid. For example, the diffusion and differential approximation methods are accurate only for large optical thickness and fail at positions near the boundaries[16]; the accuracy of the two-flux model decreases at a large optical thickness. In the solution of a transient thermal process, an accurate instantaneous temperature distribution is needed; otherwise an accumulative error will occur in the overall energy balance as time advances.

The purpose of this study is twofold. First, we present a direct numerical procedure for obtaining accurate transient temperature distribution in a semitransparent layer. The layer is emitting, absorbing, isotropically scattering, and heat conducting with a refractive index ranging from 1 to 2. The solution involves solving simultaneously the energy equation and the integral equation for the radiative flux gradient. The energy equation is solved using an implicit finite volume scheme.[17] The integral equation of radiative heat transfer is solved using the singularity subtraction technique and Gaussian quadrature.[18–20] Our second objective is to investigate the effects of isotropic scattering on the radiative cooling of a semitransparent layer. As will be seen, the scattering has a significant effect on the transient temperature distribution and the mean temperature of the layer. It is demonstrated that a direct numerical procedure can be applied without difficulty in the presence of scattering and surface reflection. Essentially, the present study attempts to extend a series of Siegel's developments.[12–14]

Analysis

Consideration is given to a plane layer of thickness D, as shown in Fig. 1. It consists of a gray medium being emitting, absorbing, isotropically scattering, and heat conducting. The layer is initially at temperature T_0 and then placed in a much colder surrounding. The dimensionless energy equation describing the system is given by[16]

$$\frac{\partial \theta}{\partial \tau} = N \frac{\partial^2 \theta}{\partial X^2} - R(\theta) \tag{1}$$

with the initial condition

$$\theta(X, 0) = 1 \tag{2}$$

Assuming the convective heat transfer is negligible such as in the space applications, the energy is then lost only by means of internal radiation passing through the surface. Note that energy can be conducted into an element layer adjacent to the surface, but energy cannot be radiated exactly from the surface that has no volume.[12] It follows that the internal conduction must decrease to zero as the surface is approached if there is no external conduction or convection. Therefore, the following boundary conditions should be used for the preceding energy equation:

$$\frac{\partial \theta(0, \tau)}{\partial X} = \frac{\partial \theta(1, \tau)}{\partial X} = 0 \tag{3}$$

In Eq. (1) $R(\theta)$ is the gradient of the radiative heat flux in the following dimensionless form[16]:

$$R(\theta) = \kappa_D(1 - \omega)[n^2\theta^4 - (\phi/4)] \tag{4}$$

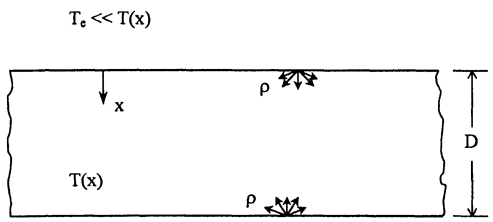

Fig. 1 Geometry and nomenclature of the plane layer.

where ϕ is the local incidence function in dimensionless form. Under the assumption of isotropic scattering, ϕ is given by

$$\phi(X) = 2\bar{J}_1 E_2(\kappa_D X) + 2\bar{J}_2 E_2[\kappa_D(1 - X)] + 2\pi\kappa_D \int_0^1 S(X')E_1(\kappa_D|X - X'|)\, dX' \tag{5}$$

where the source function $S(X)$ is given by

$$S(X) = (1 - \omega)(n^2\theta^4/\pi) + (\omega/4\pi)\phi \tag{6}$$

and $\bar{J}_1$ and $\bar{J}_2$ are the dimensionless radiosities at the two boundaries at $X = 0$ and $X = 1$, respectively. For the symmetrical case considered in this study, $\bar{J}_1 = \bar{J}_2$. Assuming that the interfaces reflect diffusively, and following Ref. 21, we obtain the expressions for $\bar{J}_1$ and $\bar{J}_2$ as

$$\bar{J}_1 = \bar{J}_2 = C/(1 - A) \tag{7}$$

where

$$A = 2\rho E_3(\kappa_D) \tag{8}$$

$$C = 2\pi\rho\kappa_D \int_0^1 S(X')E_2(\kappa_D X')\, dX' \tag{9}$$

The diffuse interface characteristics are modeled by using integrated averages of the Fresnel reflection relations. An expression of the reflectivity of the interior interface, ρ, as a function of refractive index of the layer, can be found in Ref. 16 (p. 115). Spuckler and Siegel[21] pointed out that this kind of treatment of the interfaces is a good approximation, unless the extinction coefficient is large.

Inserting Eqs. (6–9) into Eq. (5) leads to

$$\phi(X) = n^2 \int_0^1 F(X, X')\theta^4(X')\, dX' + 2n^2\kappa_D(1 - \omega) \int_0^1 \theta^4(X')E_1(\kappa_D|X - X'|)\, dX' + \frac{\omega}{4(1 - \omega)} \int_0^1 F(X, X')\phi(X')\, dX' + \frac{\omega}{2}\kappa_D \int_0^1 \phi(X')E_1(\kappa_D|X - X'|)\, dX' \tag{10}$$

where

$$F(X, X') = 4\frac{\rho\kappa_D(1 - \omega)}{1 - A}\{E_2(\kappa_D X) + E_2[\kappa_D(1 - X)]\}E_2(\kappa_D X') \tag{11}$$

Equations (1–4) and Eqs. (10) and (11) must be solved simultaneously to obtain the transient temperature distribution

across the layer. The mean temperature of the layer as a function of time is given by

$$\theta_m(\tau) = \int_0^1 \theta(X, \tau)\, dX \tag{12}$$

Solution Methodology

Energy Equation

The energy equation is discretized using the implicit finite volume scheme.[17] Because of strong nonlinearity of the radiative flux, special care must be taken on the source term, $R(\theta)$ in Eq. (1), to guarantee good convergence of the solution. To this end, we linearize $R(\theta)$ as follows:

$$R(\theta) = R(\theta^*) + \frac{dR(\theta^*)}{d\theta}(\theta - \theta^*) = R(\theta^*) - \frac{dR(\theta^*)}{d\theta}\theta^* + \frac{dR(\theta^*)}{d\theta}\theta \tag{13}$$

where θ^* is the temperature from the previous iteration. $R(\theta^*)$ and $dR(\theta^*)/d\theta$ represent R and $dR/d\theta$ evaluated in terms of θ^*.

From Eq. (4) we have

$$\frac{dR(\theta^*)}{d\theta} = \kappa_D(1 - \omega)\left(4n^2\theta^{*3} - \frac{1}{4}\frac{d\phi^*}{d\theta}\right) \tag{14}$$

and Eq. (10) gives

$$\frac{d\phi^*(X)}{d\theta} = 4n^2\int_0^1 F(X, X')\theta^{*3}(X')\, dX' + 8(1 - \omega)n^2\kappa_D\int_0^1 \theta^{*3}(X')E_1(\kappa_D|X - X'|)\, dX' + \frac{\omega}{4(1 - \omega)}\int_0^1 F(X, X')\frac{d\phi^*(X')}{d\theta}\, dX' + \frac{\omega\kappa_D}{2}\int_0^1 \frac{d\phi^*(X')}{d\theta}E_1(\kappa_D|X - X'|)\, dX' \tag{15}$$

With $R(\theta)$ handled in this way, two additional equations, i.e., Eqs. (14) and (15), must be solved to obtain $dR(\theta^*)/d\theta$. This creates a small amount of additional work because the code developed for the solution of Eq. (10) can be directly used for the solution of Eq. (15). Note that Eqs. (10) and (15) have the same form. However, linearization of $R(\theta)$ in the form of Eq. (13) leads to much faster convergence of the solution.

Radiative Flux Equation

The integral equations, Eqs. (10) and (15), are solved numerically by using the well-known Nystrom method.[22] Attention must be paid to the singularity of the exponential integral function $E_1(\kappa_D|X - X^*|)$ at $X = X^*$. The so-called singularity subtraction technique[18–20] is used here to deal with the integrals containing E_1. For example, we can rewrite

$$\int_0^1 \phi(X')E_1(\kappa_D|X - X'|)\, dX' = \int_0^1 [\phi(X') - \phi(X)]E_1(\kappa_D|X - X'|)\, dX' + \phi(X)\int_0^1 E_1(\kappa_D|X - X'|)\, dX' \tag{16}$$

The integration in the last term on the right-hand side can be evaluated exactly, i.e.,

$$\int_0^1 E_1(\kappa_D|X - X'|)\, dX' = 2 - E_2(\kappa_D X) - E_2[\kappa_D(1 - X)]$$

After this mathematical manipulation, Eqs. (10) and (15) can be readily transformed into simultaneous algebraic equations by applying quadrature rules.

Numerical Procedures and Grid Independence Analysis

The plate is divided into M increments in X with smaller ΔX near the boundaries. The integral equations, Eqs. (10) and (15), are discretized by using the Gaussian quadrature. The Gaussian abscissas and weights are calculated using the *Numerical Recipes*[22] subroutine GAULEG. Variable time increments are used with smaller time steps in the beginning of the process. At each time level, Eqs. (1) , (4), (10), (14), and (15) are solved simultaneously and iterations are performed to obtain the temperature distribution. The procedures are briefed in the following text.

For a solution at each time increment, an initial guess of the temperature distribution across the layer must be provided. Typically in this calculation, the temperature distribution at a previous time level is used for the first guess. The values of temperature at the Gaussian abscissas are obtained using cubic spline interpolation. The subroutines SPLINE and SPLINT of Ref. 22 were used for this purpose. With the temperature specified, the values of R and $dR/d\theta$ at the Gaussian abscissas are obtained from the solution of Eqs. (4), (10), (14), and (15). The exponential integral functions E_n are calculated using EXPINT of Ref. 22. The values of R and $dR/d\theta$ at the nodes for the energy equation are then calculated using the Nystrom interplation, i.e., they are computed by using Eqs. (10) and (15) as interpolation formula. With R and $dR/d\theta$ evaluated, an updated temperature distribution is obtained by the solution of Eq. (1). This process is repeated until the desired convergence is achieved. In this calculation, a convergence is attained when the relative change of temperature between two successive iterations is less than 10^{-5} at every node.

Solutions are checked against various grid densities and orders of Gaussian quadrature. It is found that the larger the optical thickness of the layer, the denser grids and the higher-order Gaussian quadratures are needed because of steep variation of the radiative flux at the boundaries. The number of quadrature points can be always less than the number of increments in X for the energy equation. For κ_D less than 20, it is found that 60 increments in X, with $\Delta X = 0.005$–0.01 near the boundaries, and a 40-point Gaussian quadrature are sufficient. For $\kappa_D = 50$, as many as 100 increments in X, with $\Delta X = 0.0025$ near the boundaries and an 80-point quadrature are necessary. Solution is also checked against the number of increments in time. It is found that the choice of $\Delta\tau = 0.01$ in the beginning of the process and then gradually increasing to $\Delta\tau = 0.05$ is sufficient.

The calculations are performed on an IBM RS/6000 station. For a typical run with 90 increments in time, 60 increments in X, and a 40-point Gaussian quadrature, it takes about 10 min to obtain the temperature distribution and the mean temperature of the layer up to $\tau = 3.0$.

Results and Discussion

Transient Temperature Distribution

The transient temperature distributions at three different time levels are presented for various combinations of refractive indices, optical thicknesses, and scattering albedos. Only the temperature across one-half of the layer is shown because of symmetry of the system. Figure 2 depicts the transient temperature distributions for a layer of $n = 1$, and Fig. 3 for $n =$

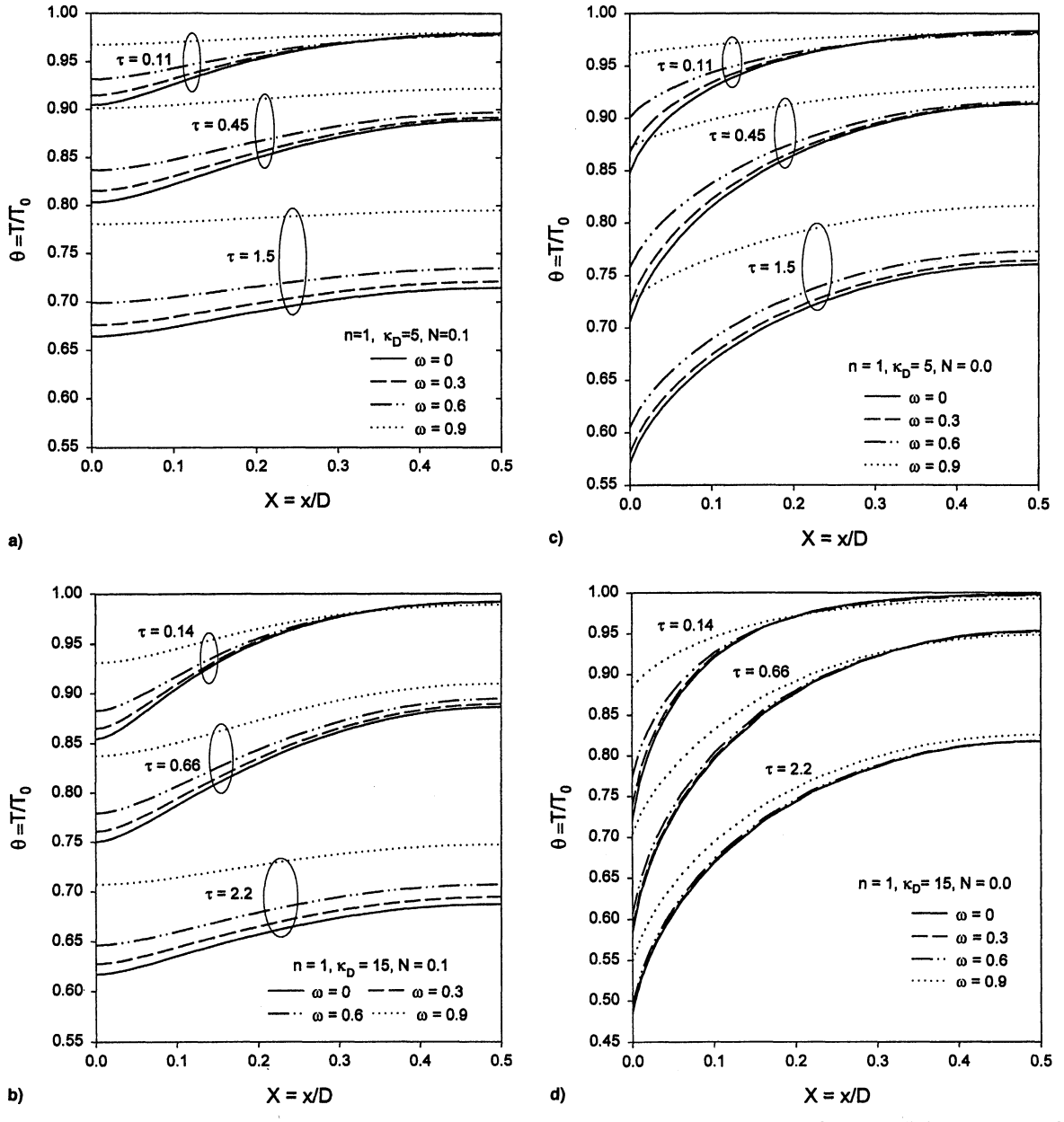

Fig. 2 Transient temperature distribution under various conditions for a layer with a) $n = 1$, $N = 0.1$, $\kappa_D = 5$; b) $n = 1$, $N = 0.1$, $\kappa_D = 15$; c) $n = 1$, $N = 0$, $\kappa_D = 5$; and d) $n = 1$, $N = 0$, $\kappa_D = 15$.

1.5, with $\omega = 0$, 0.3, 0.6, and 0.9 for all figures. The parameters κ_D, N, and the dimensionless time levels corresponding to the curves are chosen the same as those proposed in Refs. 12 and 13 for comparison purposes. The solutions for the limiting cases, i.e., obtained by letting $\omega = 0$ in the present calculation, are identical to the results of Refs. 12 and 13 and are indistinguishable from their curves. This further reinforces the numerical methods employed in this work.

Similar features to those reported by Refs. 12 and 13 are found from these curves. For example, heat conduction serves to equalize temperature across the layer; increased optical thickness gives a steeper temperature distribution near the boundaries; and a larger refractive index yields a more uniform temperature distribution.

The effect of scattering is more difficult to identify. In general, Figs. 2 and 3 show that when the optical thickness is held fixed, increasing scattering gives a more uniform temperature distribution and slows down the temperature drop. This is because of the relatively reduced emitting ability or absorption thickness of the layer, αD, when ω is increased, because the radiative heat loss of the layer depends strongly upon the magnitude of αD, which is equal to $(1 - \omega)\kappa_D$. In this case, the effect of αD is somewhat similar to that of κ_D on a nonscattering layer. In the limiting case with $\omega = 1$, the layer remains at the initial temperature because there is no emitting and absorption and, hence, no heat losses from the layer. Overall, it is found that the effect of scattering becomes significant only at larger scattering albedos. Note that at these levels of optical thickness, i.e., $\kappa_D \geq 5$, unless the value of ω is very large, i.e., very small αD, absorption is strong enough to absorb the scattered energy instead of letting it pass through the layer. Comparisons between parts a and b, and between parts c and d in Figs. 2 and 3, show that a larger optical thickness tends to weaken the effect of scattering. The reason is that a larger optical thickness and, thus, a larger absorption thickness, means more scattered energy being absorbed, which offsets the effect of scattering.

It is noticed that, in the presence of scattering, the temperature of the center layer decreases slightly faster than that without scattering at the very early stage of the transient. The curves cross at small values of τ, as can be seen in Figs. 2 and 3. This is also related to the values of αD because a smaller

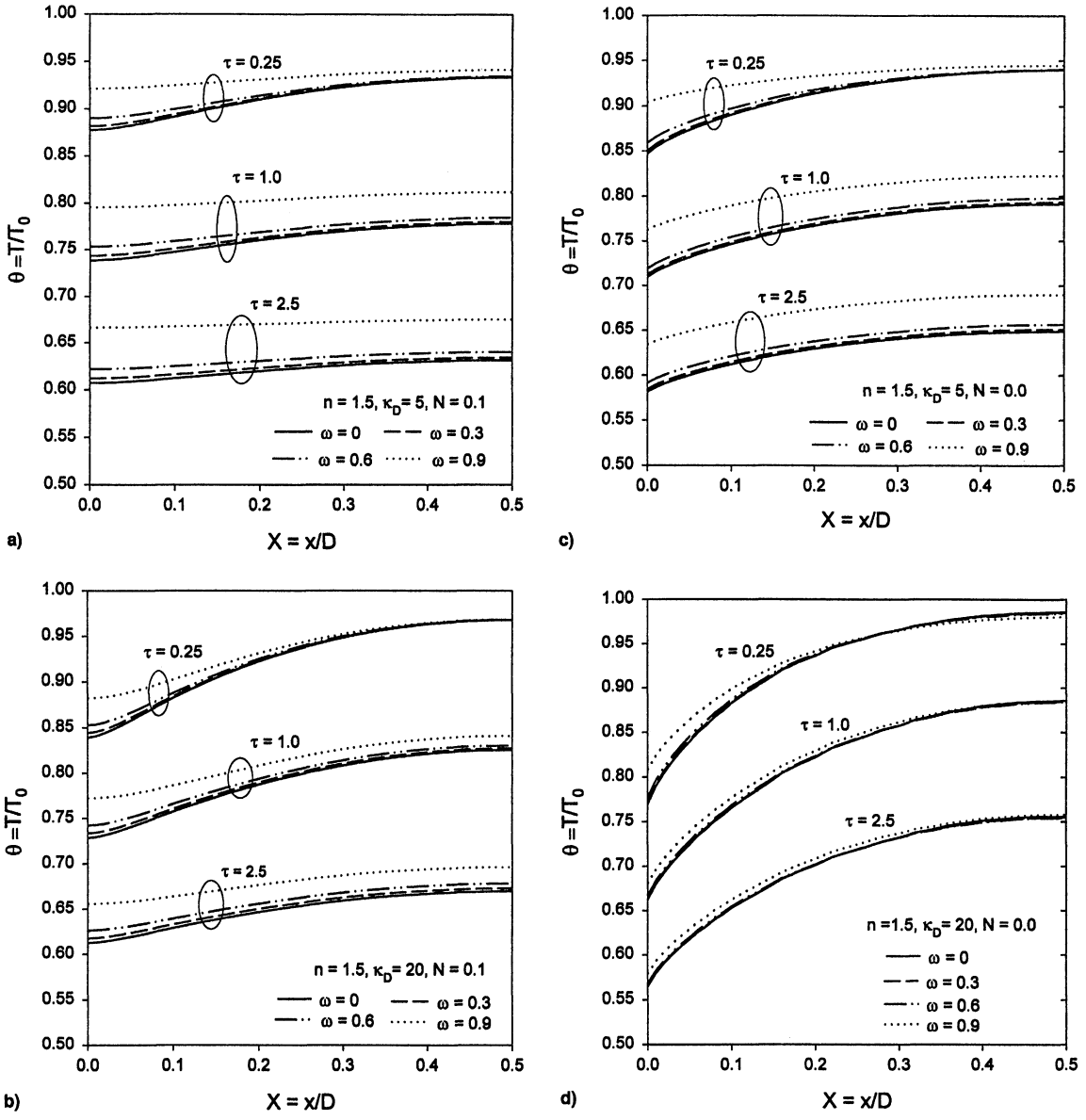

Fig. 3 Transient temperature distribution under various conditions for a layer with a) $n = 1.5$, $N = 0.1$, $\kappa_D = 5$; b) $n = 1.5$, $N = 0.1$, $\kappa_D = 20$; c) $n = 1.5$, $N = 0$, $\kappa_D = 5$; and d) $n = 1.5$, $N = 0$, $\kappa_D = 20$.

αD gives a more uniform temperature. The crossing of curves disappears gradually because the scattering layer cools more slowly than the nonscattering layer as a result of smaller αD, as explained earlier.

Transient Mean Temperature

The transient mean temperatures calculated using Eq. (12) are shown in Fig. 4 (for $n = 1$) and Fig. 5 (for $n = 1.5$), corresponding to the same choices of parameters as in parts a and b of Figs. 2 and 3. Some features discussed earlier are also reflected here.

Figures 4 and 5 clearly show that, with other conditions kept constant, increasing scattering, i.e., decreasing the value of αD, slows down the decrease of temperatures, particularly at larger scattering albedos. This is true regardless of the fact that a scattering layer has a slightly lower temperature at the center than a nonscattering layer at the early stage of the transient process. The fact that a larger optical thickness weakens the effect of scattering can be shown by a rough comparison from Fig. 4; the difference between the curve corresponding to $\omega = 0$ and the curve corresponding to $\omega = 0.9$ for $\kappa_D = 5$ is larger than that for $\kappa_D = 15$, at any time and at any temperature level.

In Figs. 4 and 5, almost all of the curves associated with $\kappa_D = 5$ are below the counterparts with $\kappa_D = 15$ and 20 because, under the chosen parameters, the temperatures near the boundaries at $\kappa_D = 15$ or 20 are much colder than the inner positions, thus reducing the cooling effectiveness of the layer, as shown in Figs. 2 and 3. However, there is an exception to this in Fig. 4; i.e., the curve corresponding to $\kappa_D = 5$, $\omega = 0.9$ is above the curve corresponding to $\kappa_D = 15$ at the same scattering level. This is because, at large scattering albedos, the behavior of mean temperature at various optical thickness is different from that at small scattering albedos, as discussed in the following text.

Effect of Large Scattering

As mentioned earlier, the effect of scattering becomes significant at large values of scattering albedos. Here we examine the effect of scattering at $\omega = 0.9$–0.99 in two different ways.

In Fig. 6, the scattering albedo is held constant at $\omega = 0.9$, but the optical thickness of the layer is varied from 2 to 50. The dependence of transient mean temperature on the optical thickness shows two different trends. At small values of κ_D, e.g., $\kappa_D < 10$, the transient mean temperature decreases with

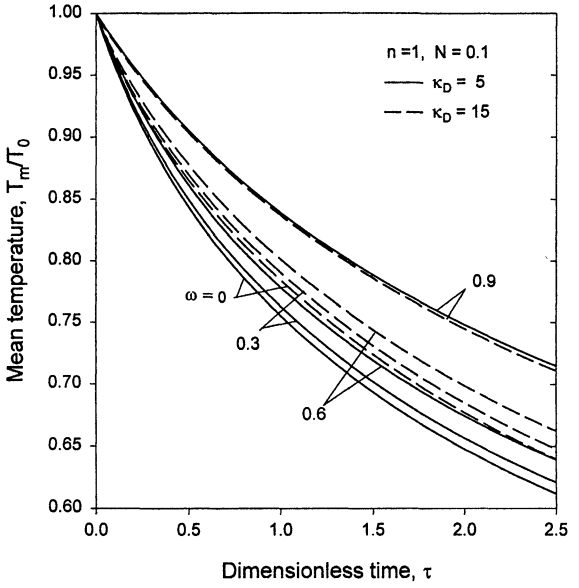

Fig. 4 Transient mean temperature of the layer of n = 1 with N = 0.1, κ_D = 5, and κ_D = 15.

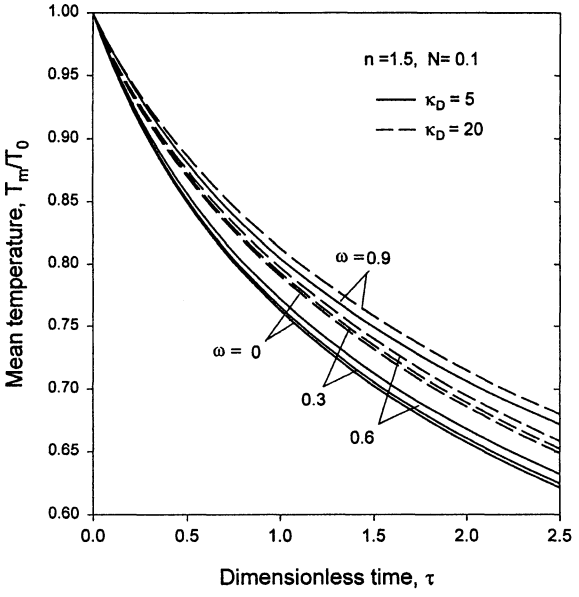

Fig. 5 Transient mean temperature of the layer of n = 1.5 with N = 0.1, κ_D = 5, and κ_D = 20.

an increasing optical thickness; however, at larger κ_D, this trend is reversed. This is related to the magnitude of αD, i.e., $(1 - \omega)\kappa_D$. When αD is small, the temperature distribution is relatively uniform, and radiation rays from the inner layer find their way to the surroundings because of relatively small absorption. In this case, increasing αD enhances the radiation and, hence, the cooling rate. On the other hand, when κ_D is large, the temperature near the boundaries becomes increasingly cooler than the interior, if the heat conduction is finite, thus reducing the cooling effectiveness of the layer. This should explain the special case appearing in Fig. 4 that was mentioned earlier. The curve for κ_D = 5, ω = 0.9, and the curve for κ_D = 15, ω = 0.9, correpond to αD = 0.5 and αD = 1.5, respectively; at such small αD, the cooling effectiveness increases with increasing αD. As a matter of fact, similar trends can be found at any values of ω, and for a layer with refractive indices larger than one, but the optical thickness around which the trend is reversed can be different, depending on the choice of such parameters as ω and N.

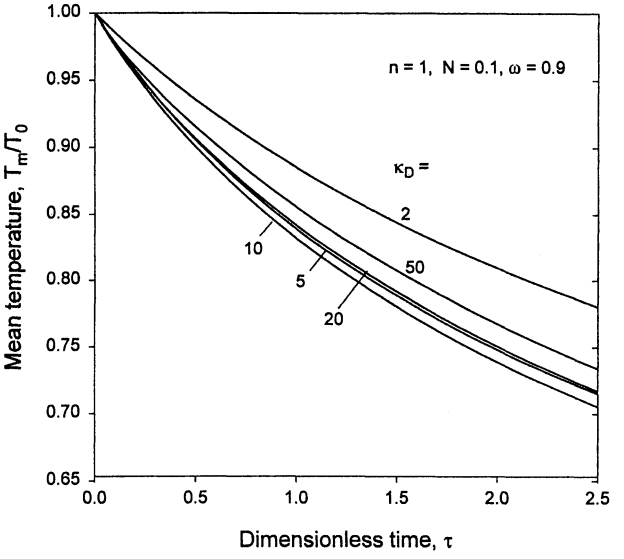

Fig. 6 Transient mean temperature of a layer of various κ_D at ω = 0.9 for n = 1, N = 0.1.

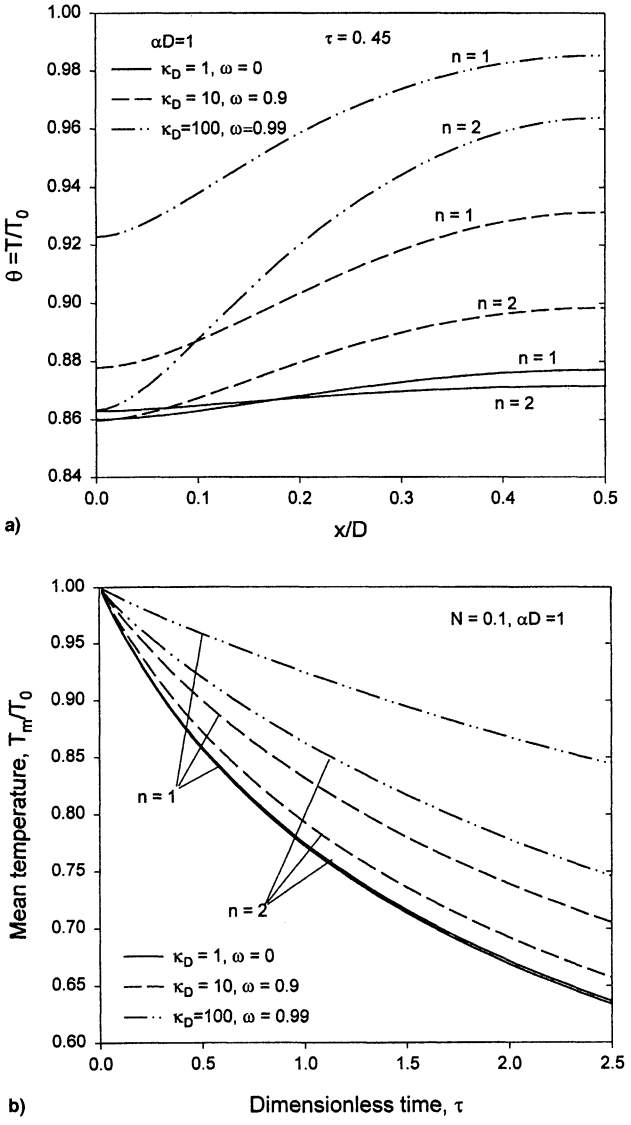

Fig. 7 Effect of increasing scattering with fixed αD = 1 for n = 1 to 2 and N = 0.1: a) temperature distribution at τ = 0.45 and b) transient mean temperature of the layer.

In Fig. 7, the effect of scattering is shown in a different way, i.e., αD is held constant, while κ_D is increased such that the effect of additional scattering can be shown. Parameters used in Fig. 7 include $N = 0.1$, $\alpha D = 1$, $n = 1$ and 2. Because $\kappa_D = \alpha D/(1 - \omega)$, in Fig. 7, $\kappa_D = 1$, 10, 100 corresponding to $\omega = 0$, 0.9, 0.99, respectively. This way of showing the effect of scattering was also discussed in Ref. 21.

The temperature distribution at $\tau = 0.45$ is shown in Fig. 7a. It is seen that increasing scattering leads to a steeper temperature distribution near the boundaries, an observation different from that shown in Figs. 2 and 3. Note that in the case of Fig. 7, κ_D is increased much faster than the increase of ω; thus the layer quickly becomes increasingly opaque. In contrast, in Figs. 2 and 3, κ_D is held constant when the effect of increasing scattering is examined. Figure 7b reflects that the cooling rate of the layer decreases with increasing ω and κ_D, with αD being fixed. This is caused by the temperature distribution depicted in Fig. 7a.

It is interesting to note the effect of refractive indices on the transient process at large scattering albedos. It has been shown in Ref. 13, which corresponds to $\omega = 0$ in the present case, that a larger n gives more uniform temperatures; and that at $N = 0.1$ and with κ_D ranging from 2 to 20, there is a decrease in the cooling rate when n is increased. These behaviors also appear in Fig. 7 and in Figs. 2 and 3 when $\omega = 0$. However, the effect of n is quite different at large ω, as is shown in Fig. 7. When $\omega = 0.9$ and 0.99, the cooling rate with $n = 2$ is considerably faster than that with $n = 1$ (see Fig. 7b), and at $\kappa_D = 100$, $\omega = 0.99$, the temperature distribution for $n = 2$ is steeper than that for $n = 1$. This is most likely a result of enhanced cooling at positions near the boundary by a combined effect of strong scattering and interface reflection.

Conclusions

A direct numerical procedure has been developed for obtaining accurate transient temperature distributions in an emitting, absorbing, isotropically scattering, and heat-conducting layer. The solution involves simultaneously solving the transient energy equation using an implicit finite volume scheme and the integral equation for the radiative heat flux using the singularity subtraction technique and Gaussian numerical quadrature. Solutions for the limiting case without scattering compare extremely well with the results available in the literature. Scattering is found to have a significant effect on the transient temperature distribution and the transient mean temperature of a layer subject to radiative cooling.

Acknowledgment

This research was supported by the Computational Mechanics Research Challenge Grant sponsored by the Ohio Board of Regents.

References

[1]Siegel, R., "Transient Thermal Effects of Radiant Energy in Translucent Materials," *Journal of Heat Transfer*, Vol. 120, No. 1, 1998, pp. 4–23.

[2]Tan, H., and Lallemand, M., "Transient Radiative-Conductive Heat Transfer in Flat Glasses Submitted to Temperature, Flux and Mixed Boundary Conditions," *International Journal of Heat and Mass Transfer*, Vol. 32, No. 5, 1989, pp. 795–810.

[3]Tan, H., Maestre, B., and Lallemand, M., "Transient and Steady-State Combined Heat Transfer in Semi-Transparent Materials Subjected to a Pulse or a Step Irradiation," *Journal of Heat Transfer*, Vol. 113, No. 1, 1991, pp. 166–173.

[4]Baek, S. W., Kim, T. Y., and Lee, J. S., "Transient Cooling of a Finite Cylindrical Medium in the Rarefied Cold Environment," *International Journal of Heat and Mass Transfer*, Vol. 36, No. 16, 1993, pp. 3949–3956.

[5]Tsai, C. F., and Nixon, G., "Transient Temperature Distribution of a Multilayer Composite Wall with Effects of Internal Thermal Radiation and Conduction," *Numerical Heat Transfer*, Vol. 10, No. 1, 1986, pp. 95–101.

[6]Hahn, O., Raether, F., Arduini-Schuster, M. C., and Fricke, J., "Transient Coupled Conductive/Radiative Heat Transfer in Absorbing, Emitting and Scattering Media: Application to Laser Flash Measurements on Ceramic Materials," *International Journal of Heat and Mass Transfer*, Vol. 40, No. 3, 1997, pp. 689–698.

[7]Diaz, L. A., and Viskanta, R., "Experiments and Analysis on the Melting of a Semi-transparent Material by Radiation," *Warme-und Stoffubertragung*, Vol. 20, No. 4, 1986, pp. 311–321.

[8]Seki, N., Sugawara, M., and Fukusako, S., "Back-Melting of a Horizontal Cloudy Ice Layer with Radiative Heating," *Journal of Heat Transfer*, Vol. 101, No. 1, 1979, pp. 90–95.

[9]Nishimura, M., Bando, Y., Kuraishi, M., and Hahne, E. W. P., "Direct Storage of Solar Thermal Energy Using a Semi-Transparent PCM—Indoor Experiment Under Constant Incidence of Radiation," *International Chemical Engineering*, Vol. 29, No. 4, 1989, pp. 722–728.

[10]Matthews, L. K., Viskanta, R., and Incropera, F. P., "Combined Conduction and Radiation Heat Transfer in Porous Materials Heated by Intense Solar Radiation," *Journal of Solar Energy Engineering*, Vol. 107, No. 1, 1985, pp. 29–34.

[11]Yuen, W. W., and Khatami, M., "Transient Radiative Heating of an Absorbing, Emitting and Scattering Material," *Journal of Thermophysics and Heat Transfer*, Vol. 4, No. 2, 1990, pp. 193–198.

[12]Siegel, R., "Finite Difference Solution for Transient Cooling of a Radiating-Conducting Semitransparent Layer," *Journal of Thermophysics and Heat Transfer*, Vol. 6, No. 1, 1992, pp. 77–83.

[13]Siegel, R., "Refractive Index Effects on Transient Cooling of a Radiating-Conducting Semitransparent Layer," *Journal of Thermophysics and Heat Transfer*, Vol. 9, No. 1, 1995, pp. 55–62.

[14]Siegel, R., "Transient Heat Transfer in a Semitransparent Radiating Layer with Boundary Convection and Reflection," *International Journal of Heat and Mass Transfer*, Vol. 39, No. 1, 1996, pp. 69–79.

[15]Siegel, R., "Two-Flux Green's Function Analysis for Transient Spectral Radiation in a Composite," *Journal of Thermophysics and Heat Transfer*, Vol. 10, No. 4, 1996, pp. 681–688.

[16]Siegel, R., and Howell, J. R., *Thermal Radiation Heat Transfer*, 3rd ed., Hemisphere, Washington, DC, 1992.

[17]Patankar, S. V., *Numerical Heat Transfer and Fluid Flow*, Hemisphere, New York, 1980.

[18]Baker, C. T. H., *The Numerical Treatment of Integral Equations*, Oxford Univ. Press, Oxford, England, UK, 1977.

[19]Crosbie, A. L., and Pattabongse, M., "Application of the Singularity Subtraction Technique to Isotropic Scattering in a Planar Layer," *Journal of Quantitative Spectroscopy and Radiative Transfer*, Vol. 34, No. 6, 1985, pp. 473–485.

[20]Crosbie, A. L., and Pattabongse, M., "Transient Conductive and Radiative Transfer in a Planar Layer with Arrhenius Heat Generation," *Journal of Quantitative Spectroscopy and Radiative Transfer*, Vol. 37, No. 4, 1987, pp. 319–329.

[21]Spuckler, C. M., and Siegel, R., "Refractive Index and Scattering Effects on Radiative Behavior of a Semitransparent Layer," *Journal of Thermophysics and Heat Transfer*, Vol. 7, No. 2, 1993, pp. 303–310.

[22]Press, W. H., Teukolsky, S. A., Vetterling, W. T., and Flannery, B. P., *Numerical Recipes in Fortran*, 2nd ed., Cambridge Univ. Press, New York, 1992.